International Journal of Design & Nature and Ecodynamics
Vol. 21, No. 7, July, 2026, pp. 2121-2131
Journal homepage: http://iieta.org/journals/ijdne

Methyl Gallate Inhibits Growth, Biofilm Formation, Enterobactin Production, and *ent* Gene Expression in Uropathogenic *Escherichia coli* Isolates

Basam Basim Mohammed[1], Afrah A. Ajeel[2], Mohammed T. Abdul Hussein[1], Enaam H. Batah[1], Tamara Abbas Hamed[1*], Maha M. Khadim[1]

[1] Department of Microbiology, College of Science, Mustansiriyah University, Baghdad 10001, Iraq
[2] Department of Biology, College of Science, Mustansiriyah University, Baghdad 10001, Iraq

Corresponding Author Email: tamara.a@uomustansiriyah.edu.iq

https://doi.org/10.18280/ijdne.210724

Received: 19 May 2026
Revised: 18 July 2026
Accepted: 25 July 2026
Available online: 31 July 2026

Keywords:
Escherichia coli, enterobactin, real-time polymerase chain reaction, antibiofilm assay, lactate dehydrogenase assay, entA, entB, entC, entD, entE, entF.

ABSTRACT

Urinary tract infections (UTIs) in Iraq are primarily caused by Uropathogenic *Escherichia coli* (UPEC), with studies showing high prevalence rates among clinical urine samples, ranging from about 30% to over 50%. The study aims to synthesize methyl gallate (MG) and investigate its antibacterial activity against isolates of uropathogenic *Escherichia coli* (*E. coli*) and its enterobactin production. Molecular characterization was used to identify the isolates, and real-time polymerase chain reaction (PCR) was used to examine the production and expression of enterobactin following MG treatment. In addition, MG was studied for its antibiofilm activity in vitro and in vivo by lactate dehydrogenase (LDH) assay and nucleic acid leakage assay. MG synthesis was verified by the Fourier transform infrared (FTIR) spectrum analyses. Approximately six of the ten isolates were found to be strains of presumptive *E. coli*. For MG, the minimum inhibitory concentration (MIC) was determined to be 76.23 µg/mL and MG decreased biofilm development by 31% after 12 h and by 76% after 24 h at the subinhibitory concentration (1/2 MIC) ($p < 0.05$). Both the LDH activity and the enterobactin content were found to be decreased on treatment with ¼ MIC and ½ MIC ($p < 0.05$). Following treatment with MG at ½ MIC, we discovered that all six gene members (*entA*, *entB*, *entC*, *entD*, *entE* and *entF*) exhibited significant downregulation ($p < 0.05$). In our investigation, MG shows great promise as an antibacterial agent to prevent *E. coli* from surviving. It may also function as a powerful naturally occurring bioactive substance that can lower bacterial viability and biofilm formation.

1. INTRODUCTION

With an expected 400 million cases and 230,000 fatalities globally in 2019, urinary tract infections (UTIs) are the most prevalent among bacterial illnesses [1]. As per the census, more than half of the female population suffers from a UTI during their lifetime. Additionally, UTIs rank second, next to respiratory infections, among hospitalized patients, making them one of the most prevalent infections among older people [1, 2]. Uropathogenic *Escherichia coli* (UPEC) infection is the leading cause of UTIs, accounting for 65% of severe UTIs and 75% of uncomplicated UTIs. UPEC is a member of the extraintestinal pathogenic *Escherichia coli* (ExPEC) group of pathogenic *Escherichia coli* (*E. coli*), which consists of four pathotypes that are categorized according to the site of isolation. All of these pathotypes seem to develop virulence mechanisms, which make the strains multiply and cause systemic symptoms in the host [3]. The infection commences when the bacteria residing in the stomach enter the urethra by colonizing the epithelial cells and slowly colonize the bladder. This series of processes is responsible for the host's innate immunological response to infection. Pattern recognition receptors (PRRs) like toll-like receptors (TLRs) and pathogen-associated molecular patterns (PAMPs) are very crucial in this reaction [4, 5].

There are many virulence factors that aid in forming biofilms, making the UPEC strains able to colonize the bladder and gain resistance to standard antibiotic therapy [6, 7]. Adhesion factors like type 1 fimbriae, P fimbriae, curli fibers, S fimbriae, F1C fimbriae, Dr fimbriae, afimbrial adhesins, and PapC are among them. Adhesion factors enable UPEC to colonize the urinary tract and adhere to host cells to avoid the host immune response [8, 9]. Additionally, apart from causing tissue damage, toxins like α-hemolysin and serine protease autotransporters induce morphological alterations within the host cells, promoting bacterial persistence [10]. Furthermore, siderophore-iron transporter proteins also aid in absorbing iron [11]. In the urinary system, when there is an iron-limited environment, these help UPEC to scavenge iron and enhance bacterial growth and survival [12].

Bacteria release siderophores, like enterobactin, to scavenge iron from their surroundings. *E. coli* and other gut microbes release enterobactin, which is said to be the strongest iron chelator because of its strong attraction for ferric iron [13]. Enterobactin allows pathogens to multiply in iron-limited host settings (gut and bloodstream) by binding iron and

transporting it back to the bacteria. As this iron uptake is closely associated with producing several virulence factors to elude host immune defenses, this ability not only promotes bacterial growth but also increases their pathogenicity towards the host [14]. The clinical significance of *E. coli* and other intestinal infections cannot be overstated. *E. coli* causes UTIs, sepsis, and diarrheal diseases, particularly in developing countries [15]. Additionally, the rising prevalence of multidrug-resistant (MDR) strains of *E. coli* and the illnesses is now calling for novel therapeutic and preventive measures.

Some naturally derived phenolic compounds, especially methyl gallate (MG), might reduce dependence on conventional antibiotics by inhibiting bacterial growth. Targeting virulence factors, such as enterobactin, is a viable approach to combat these infections [16]. Unlike traditional antibiotics, which either kill or restrict bacterial growth and often lead to the evolution of resistance, targeting virulence factors aims to disarm pathogens without directly providing selective pressure for resistance. This strategy not only lessens bacterial pathogenicity but also safeguards the host microbiome and reduces the chance that resistance may develop [17]. Enterobactin is produced via a biosynthetic pathway that includes many genes and enzymatic steps [18], and the six genes that make up *E. coli*'s ent (enterobactin) operon include *entA*, *entB*, *entC*, *entD*, *entE*, and *entF*. All of these encode enzymes necessary for the synthesis of enterobactin. These enzymes work together to convert chorismate, a common precursor generated by the shikimate pathway, into the complete enterobactin molecule.

The process begins when chorismate is converted to isochorismate, which is catalyzed by isochorismate synthase (*entC*). Next, isochorismatase (*entB*) converts isochorismate to 2,3-dihydro-2,3-dihydroxybenzoate (DHB), an essential pathway intermediate. Furthermore, *entB* binds DHB for subsequent stages, acting as a carrier protein. This 2,3-dihydroxybenzoate-AMP ligase (*entE*) produces DHB-AMP by adenylating DHB. This active intermediate is necessary for enterotoxin assembly. Three DHB molecules are assembled into the cyclic trilactone structure of enterotoxin during the latter stages, and this enterobactin synthase complex, which includes *entD*, *entE*, and *entF*, catalyzes this activity.

EntD is a phosphopantetheinyl transferase that modifies *entB* and *entF* so that they may act as carrier proteins. The nonribosomal peptide synthetase (NRPS) *entF* helps DHB molecules condense and cyclize into enterobactin [19]. Since enterobactin is essential to bacterial iron uptake, it is a prospective target for the creation of new antibiotics. Enterobactin-deficient bacterial strains have been employed in a number of investigations to investigate pathogenicity, stress responses, and iron uptake. The Δ*entA* mutant of Pectobacterium atrosepticum demonstrated decreased oxidative stress resistance and virulence in plants primed with salicylic acid, underscoring enterobactin's function as a conditional virulence factor [20]. Similarly, research employing uropathogenic *E. coli* CFT073 showed that altered enterobactin pathways might be employed to deliver antibiotics specifically through enterobactin receptors [21].

This study synthesized MG and evaluated its antibacterial activity against UPEC isolates, with particular emphasis on enterobactin production and its role in bacterial virulence and cell viability. The study also investigated the potential correlation between enterotoxin-associated proteins and the survival ability of UPEC under MG treatment to assess the therapeutic potential of siderophore-targeted strategies in reducing bacterial virulence and stress adaptation.

2. MATERIALS AND METHODS

2.1 Ethical approval

Urine samples were collected following approval from the Institutional Ethics Committee of Mustansiriyah University (Approval No. BCSMU/1026/000106M). Written informed consent was obtained from participants. Samples were anonymized before laboratory processing. All bacterial procedures were conducted according to institutional biosafety guidelines.

2.2 Study population

The study population is composed of patients who visited Alkendi Hospital in Iraq. Twenty untreated outpatients with symptoms of UTIs were included in this investigation, which was conducted during that time. Clinical urine samples were collected from the study subjects. The present investigation did not include subjects who had received treatment in the past.

2.3 Methyl gallate preparation

MG was produced by reacting gallic acid (Qualigens) with methanol (molecular grade, Qualigens). The contents were mixed thoroughly and boiled until a white precipitate was formed, which was MG. The reaction conditions included gallic acid (20 mg/mL) added to 50 mL of absolute methanol at 37 °C for 24 h. The white powder formed was filtered and pulverized. The MG formed was further characterized with Fourier transform infrared (FTIR) compared with MG standard samples [22].

2.4 Characterization of the methyl gallate

The MG was successfully synthesized with a yield percentage of 85%. An ultraviolet-visible (UV-VIS) spectrophotometer (Shimadzu, 1800) with a resolution of 1 nm between 200 and 800 nm was employed to measure the UV-VIS spectrum in an aqueous solution to confirm the production of MG. FTIR spectra were obtained employing the KBr pellet method on a single FTIR spectrophotometer (Bomem MB100) with a 4000–500 cm^{-1} range. MG and the extracted enterobactin were both subjected to FTIR characterization.

2.5 Molecular characterization of the isolates

Following sterile processing, the clinical samples obtained from the study population were quickly sent to the laboratory for examination. After that, the urine sample was inoculated onto MacConkey agar and allowed to grow for 24 to 48 h at 37 °C. Isolates tested gram positive were excluded, and ten out of 20 were tested as Gram-negative. The genomic DNA of all ten bacterial isolates was extracted, and 16S rRNA primers (FW: 5'-AGTTTGATCGTGGCTCAG-3'; RV: 5'-GGACTACCAGGGTATCTAAT-3') were used to amplify the strain-specific 16S rRNA subunit in a thermal cycler. Primers were acquired from Eurofins, Bangalore, India, and were created employing Primer3 software [23, 24]. The program of the polymerase chain reaction (PCR) included

initial denaturation at 95 ℃ for 5 min, denaturation at 94 ℃ for 30 s, annealing at 55 ℃ for 40 s, extension at 72 ℃ for 55 s, and final extension at 72 ℃ for 10 min. Purification and sequencing were performed on the amplified PCR products. The sequences of the ten isolates were subjected to BLAST analysis employing the NCBI BLAST program at www.ncbi.nlm.nih.gov. 1.5% agarose gel electrophoresis was utilized to analyze the PCR products, and GEL DOC (GENEI) UV trans illuminator was employed to observe the results.

2.6 Determination of the minimum inhibitory concentration

The antibacterial potential of MG was assessed by the microdilution technique, following the instructions of the Clinical and Laboratory Standards Institute (CLSI), to determine the minimum inhibitory concentration (MIC). For the MIC assay, varying concentrations (5, 10, 20, 40, or 80 µg) of MG dissolved in 10% dimethyl sulfoxide (DMSO) (1 mg/mL) were employed to treat *the E. coli* culture. About 10 µL of overnight bacterial isolate was added to all the wells loaded with 180 µL of Mueller-Hinton broth (MHB). The endpoint was identified by the absence of turbidity in the wells. The plates were incubated at 37 ℃ for 24 h, and following that, turbidity was measured at 590 nm, employing a microplate reader. Ciprofloxacin (1 mg/mL) was utilized as a positive control (PC).

2.7 Biofilm inhibition assay

According to Irayyif et al. [25], biofilm inhibition was performed. A 96-well microtiter plate was filled with 180 µL of MHB and 10 µL of bacterial culture. Microtiter plates were incubated at 37 ℃ for 24 to 48 h after MG at different doses (¼ MIC and ½ MIC) was added to each well. Following the incubation period, 200 µL of 70% glacial acetic acid was loaded onto the plates together with 0.1% crystal violet to recover the stain that had been absorbed. A plate reader (Genetix Ltd.) was employed to measure absorbance at 595 nm. At both ¼ and ½ MIC, ciprofloxacin (MIC) was utilized as a PC.

2.8 Nucleic acid leakage assay

The assay was performed following the protocol described by Oh et al. [26] with minor modifications. Overnight-grown bacterial cultures (2 mL) were treated with MG at sub-inhibitory concentrations (¼ MIC and ½ MIC). Treatments were applied at defined intervals (4 h and 8 h). After incubation, the cell suspensions were passed through Hi-Media filters (25 mm, 0.2 µm pore size) to remove the intact cells. The filtrates obtained were then recorded for absorbance at 260 nm employing a UV-VIS spectrophotometer (Shimadzu 1800) to quantify the amount of nucleic acid release.

2.9 Lactate dehydrogenase assay

The lactate dehydrogenase (LDH) kit was adapted as a biochemical indicator of membrane-associated enzyme leakage. Membrane damage in *E. coli* exposed to MG was assessed employing a commercial LDH assay kit. Bacterial cultures were incubated with MG at sub-inhibitory concentrations (¼ MIC and ½ MIC) for 8 h at 37 ℃, following the procedure described by Venkatasubbu et al. [27]. The assay was carried out as per the manual. Absorbance values were recorded at 490 nm and 690 nm employing a spectrophotometer. The percentage of LDH release was calculated employing the formula:

$$\frac{LDH\ from\ Sample\ -\ LDH\ in\ Media}{Max\ LDH\ after\ cell\ lysis\ -\ LDH\ from\ sample} \times 100 \quad (1)$$

2.10 Enterobactin production

A single colony of *E. coli* was added to 5.64 grams of M9 minimal medium suspended in 100 mL of water, and the mixture was shaken at 150 rpm for 24 to 48 h at 37 ℃ [28, 29]. The isolates were cultured at varying concentrations (1/4 MIC and ½ MIC) of MG. The culture was centrifuged for 10 min at 6,000 rpm after incubation, and the supernatant was collected. After that, the supernatant was acidified with strong HCl (pH ~2.0) and sterilized through a 0.22 µm filter. To split the contents into phases, an aliquot of ethyl acetate was added and thoroughly stirred. A rotary evaporator was used to collect and evaporate the top organic phase that contained the enterobactin. For quantification, the dried extract was diluted in 70% methanol and employed for quantification. About 0.5 mL of HCl (0.5 N) was added to around 0.5 mL of the enterobactin solution, and after mixing the components, 0.5 mL of nitrite-molybdate reagent (sodium nitrite and sodium molybdate in water) was added. To the contents, 0.5 mL of 1N NaOH was added after gently mixing, and the mixture was then incubated until a crimson color appeared. Next, absorbance was measured at 515 nm. The 2,3-dihydroxybenzoic acid (DHB) was employed to create the standard curve.

2.11 Quantitative real-time polymerase chain reaction

RNA was extracted employing the RNeasy kit following the manufacturer's instructions. The SuperScript TMII Reverse Transcriptase, 200 U/l (HiMedia) reverse transcription-polymerase chain reaction (RT-PCR) kit was used to create the cDNA. About 1 µL of cDNA, 5 µL of HiMedia SYBR Green PCR master mix, and 0.5 µM specific primers were utilized in each qRT-PCR reaction. Denaturation at 95 ℃ for 5 min, 40 cycles of denaturation at 95 ℃ for 20 s, annealing at 58 ℃ for 40 s, and extension at 72 ℃ for 20 s comprised the reaction cycle. Primers are listed in Table 1. The control and treatment samples were quantified in real time employing the Corbett Research cycler (Bio-Rad). The real-time PCR technology was employed to quantify the *entA, entB, entC, entD, entE,* and *entF* genes. To compare the mRNA expression, the relevant genes of interest and the housekeeping gene *gyrA* were amplified. The relative amounts of mRNA in the test samples and the control were compared employing the $\Delta\Delta^{Ct}$ technique.

2.12 Statistical analysis

The Statistical Package for the Social Sciences (SPSS; Faculty version) was used for analysis throughout the investigation. Data were expressed as mean ± standard deviation (SD). Differences among groups were analyzed using one-way analysis of variance (ANOVA), followed by Tukey's multiple comparisons test at $p < 0.05$.

Table 1. List of primers employed for the study

Gene	GC%	Primer Nucleotide Sequence (5' to 3')	Tm	Ref.
entA	55 50	TGA AAC GGA GCG ACT GGA C AAA CCA CAT TAC AGC GCA CG	60	[18]
entB	55 55	TAC GCA CTG CCG GAG TCT CAC CCG GCC ACA TAT TTC AGC GACA	60.0	
entC	54 55	CGT TTT ACC CGC AGC CAG TCG ACA ATG CCG CCA AAC AGT TCG	60.7	
entD	50 55	CAC AAC TGC AAC ACG CTG GAC TCT CAC TTG CCT TAA ATG CGC TCT	58.6	
entE	55 55	CCA CTG ACC GAC ATT CTG ACT GTT ATG CTC ACC GCT GTC GTT	59.0	
entF	55 55	CCG CTG CAA CTT TCA CAA CCG ATA GAG ATC ACC CGC CAC ACC	60.4	
gyrA	55 54	GTCGTGGCGGGAAAGGTAAA CGGCTGGAGAAGCACAGAA	62	[30]

Note: Tm: melting temperature; Ref.: Reference.

3. RESULTS

3.1 Characterization of methyl gallate

The FTIR spectrum (Figure 1) revealed strong bands between 3494 and 3285 cm^{-1}, corresponding to O–H stretching vibrations typical of phenolic groups. Bands in the range of 2994–2962 cm^{-1} depict C–H stretching of aromatic and methyl groups, while sharp bands observed between 1715 and 1681 cm^{-1} correspond to carbonyl (C = O) stretching. Also, the bands between 1612 and 1590 cm^{-1} depict C = C stretching within aromatic rings and were found to be consistent. From the UV spectra, it was observed that a strong peak at 270 nm was found to be shifted to 275 nm upon synthesis of MG.

FTIR spectra revealed absorption bands of enterobactin. The broadband region of 3000–3500 cm^{-1} corresponds to overlapping O–H and N–H stretching vibrations (Figure 2), while the band at 1690 cm^{-1} corresponds to amide carbonyl groups. The peaks observed at 1607 and 1532 cm^{-1} represent C = C stretching and C–H bending overlaps, respectively. Peaks between 1000 and 1000–1300 cm^{-1} were associated with C–OH, C–H, N–H, and O–H functional groups.

3.2 Identification of bacteria

The UPEC was identified by colony morphology, Gram staining, and biochemical tests. The biochemical tests revealed indole positive, methyl red positive, citrate negative, and urease negative. Out of the 20 urine samples analysed (Table 2), 14 were obtained from male patients and 6 from female patients. Among the positive isolates, only Gram-negative bacteria were considered for further screening. Within this group, 6 of the 10 isolates were identified as *E. coli* strains. The amplified product (258 bp) was sequenced. The FASTA sequence analysis revealed that the strains were 97.29% similar to *E. coli* (Acc. No.: LC844818.1) (Sequence coverage of 100% and e-value of 2e-118).

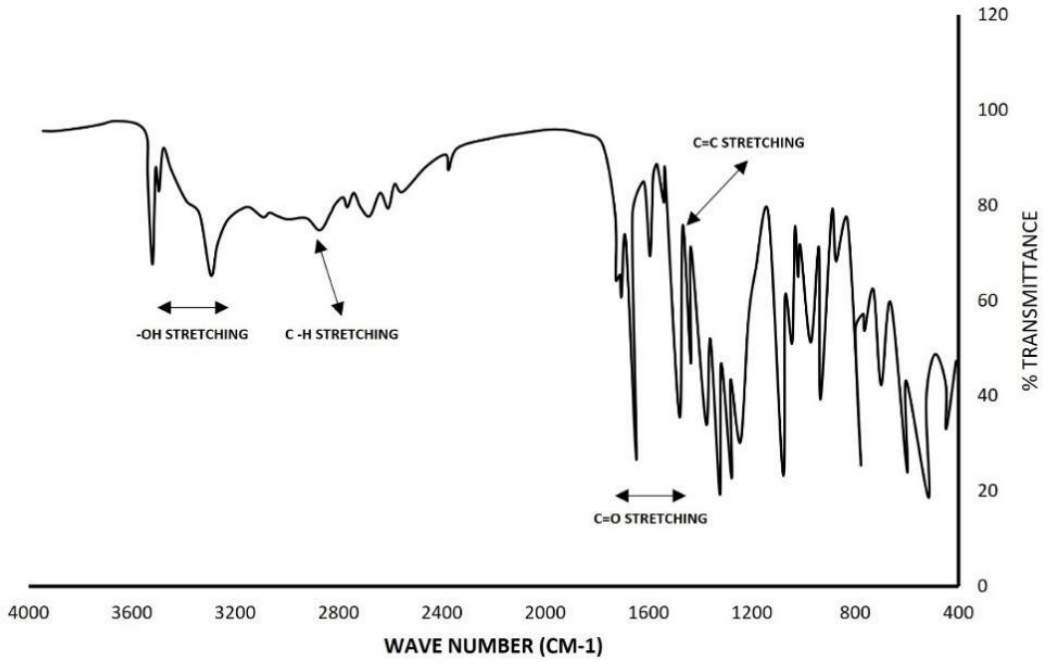

(A)

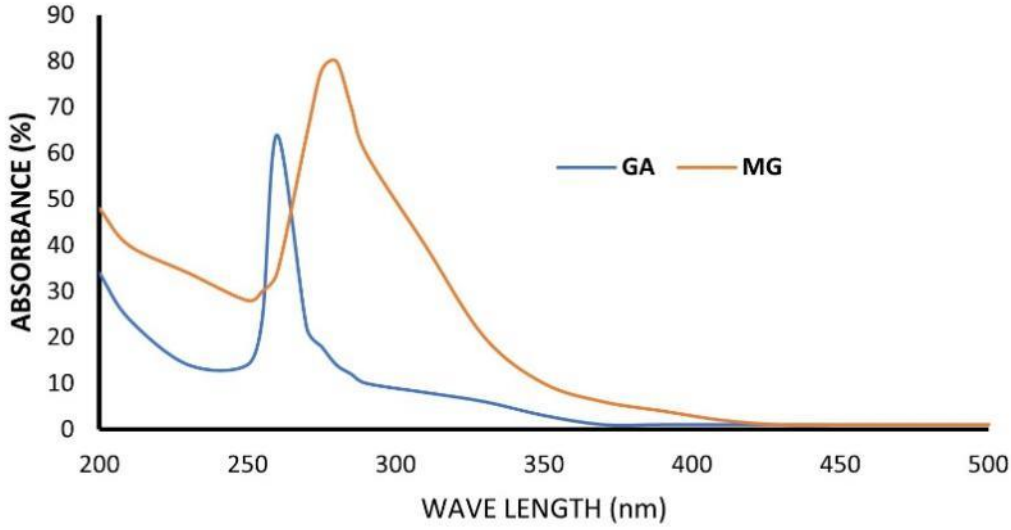

(B)

Figure 1. (A) Fourier transform infrared (FTIR) spectra of methyl gallate (MG); (B) UV spectra of gallic acid (GA) and MG

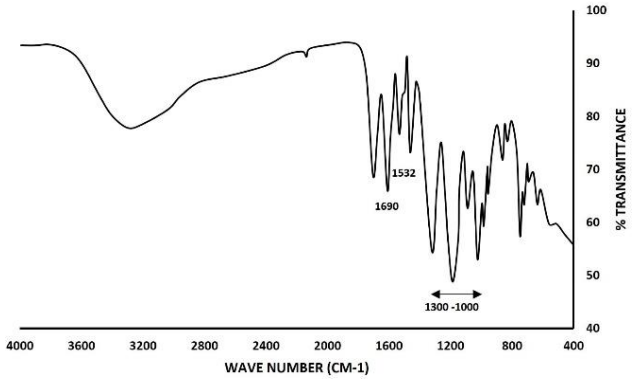

Figure 2. Fourier transform infrared (FTIR) spectra of the extracted enterobactin

Table 2. Clinical sample processing workflow

Step	Number
Urine samples collected	20
Male patients	14
Female patients	6
Positive bacterial cultures	9
Gram-negative isolates selected	6
Presumptive UPEC isolates	6

Note: UPEC = uropathogenic *Escherichia coli*.

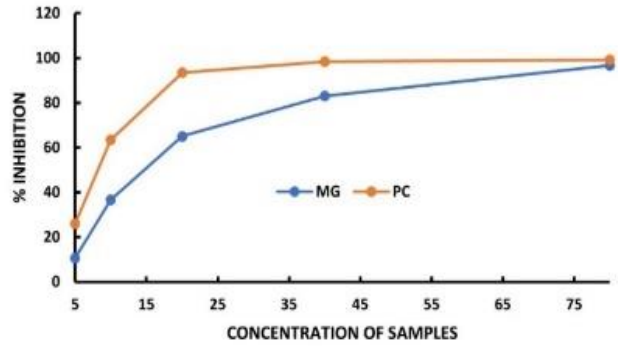

Figure 3. Percentage inhibition in bacterial growth following treatment with methyl gallate (MG) and ciprofloxacin positive control (PC)

3.3 Minimum inhibitory concentration of methyl gallate

Treatment with MG produced a marked inhibition of bacterial growth. At a concentration of 76 µg/mL, growth inhibition reached 97%, which was statistically significant compared to the PC at 40 µg/mL ($p < 0.05$), as shown in Figure 3. The MIC (minimum inhibitory concentration) was calculated to be 76.23 µg/ml for MG and 61.19 µg/ml for the PC, both values showing significance at $p < 0.05$.

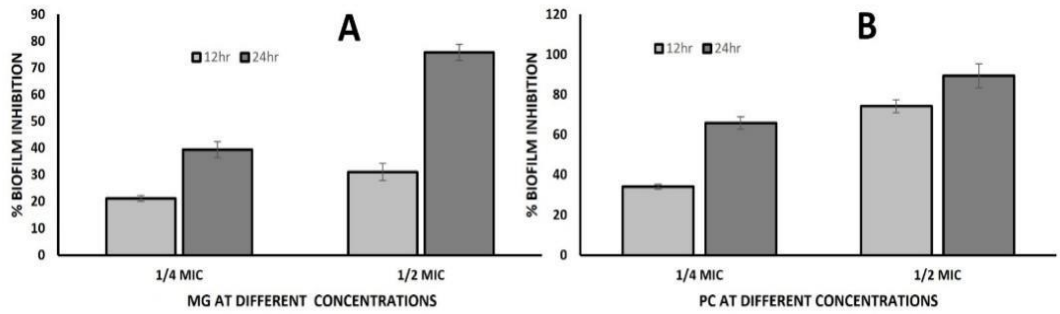

Figure 4. Percentage inhibition in biofilm formation: (A) methyl gallate (MG); (B) positive control (PC)
Note: $p < 0.05$.

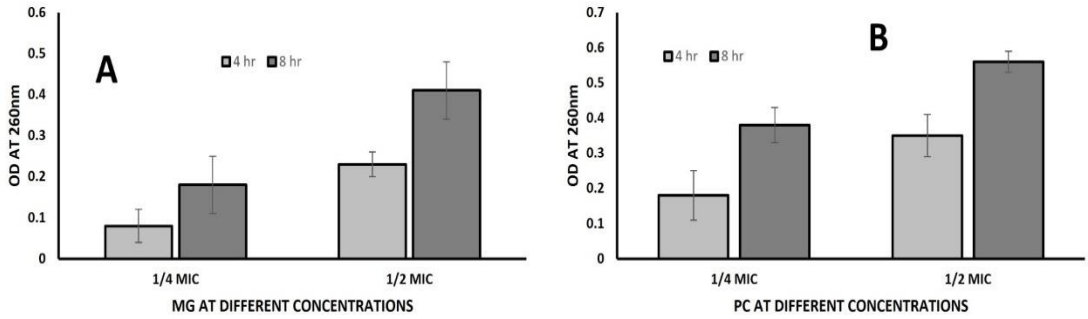

Figure 5. Nucleic acid leakage assay as measured at 260 nm: (A) methyl gallate (MG); (B) positive control (PC)
Note: $p < 0.05$.

3.4 Biofilm inhibitory potential of methyl gallate

At the sub-inhibitory concentration (1/2 MIC), MG reduced biofilm formation by 31% after 12 h and by 76% after 24 h ($p < 0.05$). In comparison, the PC exhibited 74% and 89% inhibition (Figure 4) at the same time points ($p < 0.05$). The inhibitory effect of MG was both dose-dependent and time-dependent, with statistical significance observed across treatments ($p < 0.05$).

3.5 Influence of methyl gallate on nucleic acid leakage

Leakage of nucleic acids from *E. coli* cells exposed to MG was evaluated by measuring absorbance at 260 nm in cell-free filtrates. At the start of incubation, neither MG-treated cells nor controls showed detectable leakage. After 8 h of exposure, absorbance values increased significantly from 0.18 ± 0.05 to 0.41 ± 0.07 at ¼ MIC and ½ MIC concentrations of MG, respectively ($p < 0.05$), as shown in Figure 5. In comparison, the PC exhibited an increase from 0.38 ± 0.04 to 0.56 ± 0.03 under the same conditions ($p < 0.05$). Filtrates from untreated cultures consistently showed lower nucleic acid levels than those from MG-treated cells, confirming that MG exposure compromised membrane integrity.

3.6 Effect of methyl gallate on oxidative stress-induced damage in cell respiration

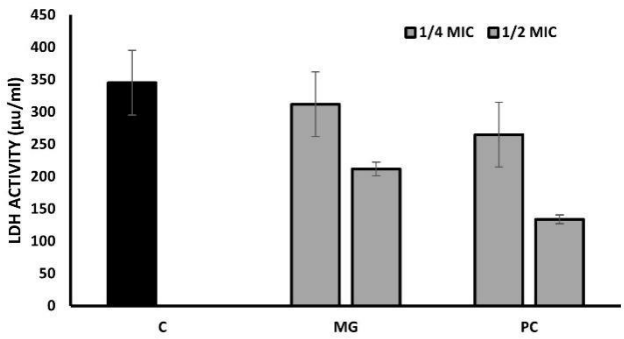

Figure 6. Effects of methyl gallate (MG) on lactate dehydrogenase (LDH) activity for 12 h
Note: PC = positive control.

To determine the effect of MG on oxidative stress-induced damage in cellular respiration, the activity of LDH, a reliable marker for determining cell status under oxidative and heat stress conditions, was measured. The effects of MG at varying concentrations on LDH activity of *E. coli* isolates are shown in Figure 6. The *E. coli* control group showed 345 µU/mL, while the LDH activities of the MG-treated cells showed a reduction in activity ($p < 0.05$). MG showed 312 and 210.5 µU/mL, respectively, at ¼ MIC and ½ MIC ($p < 0.05$). On the other hand, PC showed 265 and 134 µU/mL at ¼ MIC and ½ MIC, respectively ($p < 0.05$). It was also observed that *E. coli* cells were susceptible to MG treatment compared to PC ($p < 0.05$), as depicted in Figure 6.

3.7 Estimation of enterobactin

From the standard curve ($Y = 0.365x + 0.0506$; $R^2 = 0.9928$), a significant difference in the amounts of extracellular catechols detected upon treatment with varying concentrations of MG was observed. It was found that the enterobactin content was reduced to 1.825 ± 0.41 with MG at ½ MIC ($p < 0.05$) from 2.23 ± 0.14 (control). On the other hand, the PC showed 1.092 ± 0.27 at ½ MIC concentration ($p < 0.05$) as depicted in Figure 7. This confirms the possible role of MG in inhibiting bacterial growth.

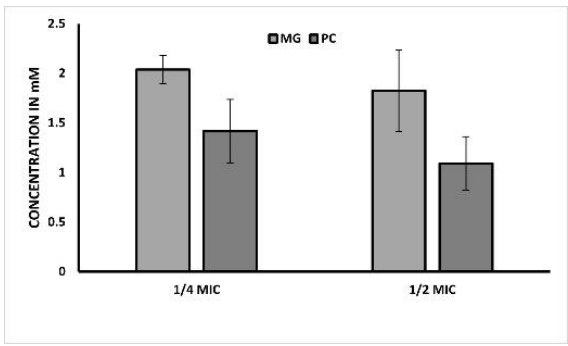

Figure 7. Level of enterobactin following the treatment of methyl gallate (MG) and positive control (PC)
Note: $p < 0.05$.

3.8 Influence of methyl gallate on gene expression

Gene expression was performed employing real-time PCR to quantify the levels of *entA* (Figure 8(A)), *entB* (Figure 8(B)), *entC* (Figure 8(C)), *entD* (Figure 8(D)), *entE* (Figure 8(E)), and *entF* (Figure 8(F)). All six gene members showed downregulation following treatment with MG at ½ MIC ($p < 0.05$). Specifically, *entA* expression decreased to 0.88 with MG and 0.92 with the PC ($p < 0.05$). Similarly, *entB* was reduced to 0.95 and 0.96, *entC* to 0.84 and 0.88, *entD* to 0.79 and 0.82, *entE* to 0.88 and 0.92, and *entF* to 0.79 and 0.86 for MG and the PC, respectively ($p < 0.05$), as mentioned in Figure 9. These findings confirm that MG at ½ MIC exerts a

broad inhibitory effect on biofilm-associated gene expression. Mel curve analysis was used to verify the purity and specificity of real-time PCR primers. There were no primer dimers and non-specific products during the Ct curve generation, validating the high reliability of the primer sets.

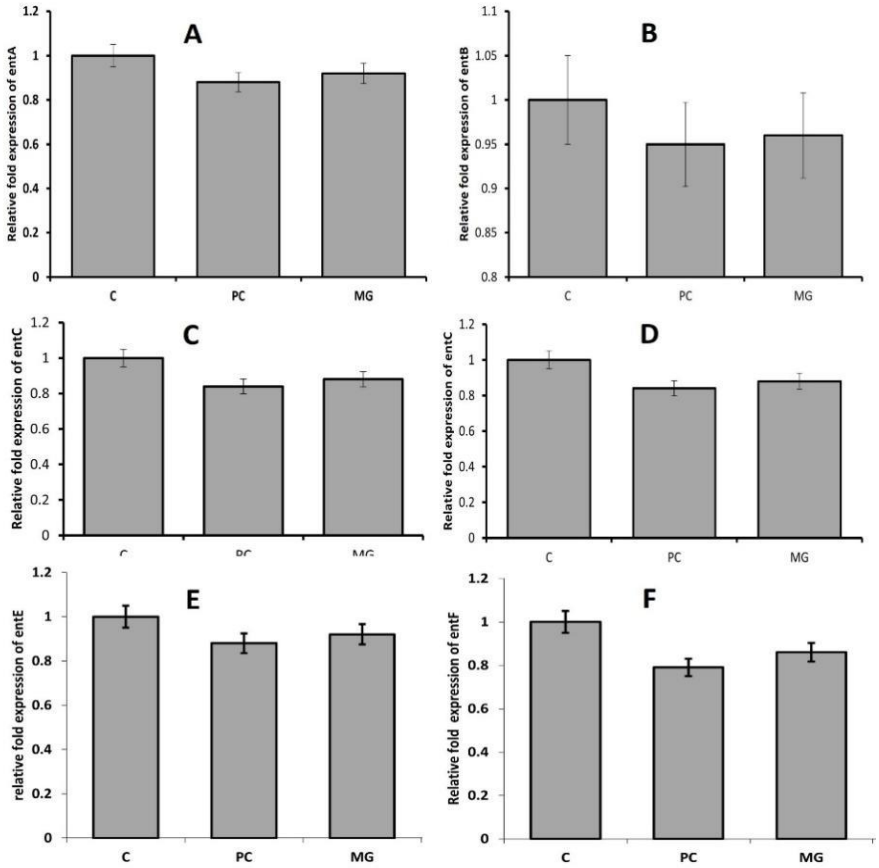

Figure 8. Histogram showing the fold expression of the gene members in the study: (A) *entA*; (B) *entB*; (C) *entC*; (D) *entD*; (E) *entE*; (F) *entF*

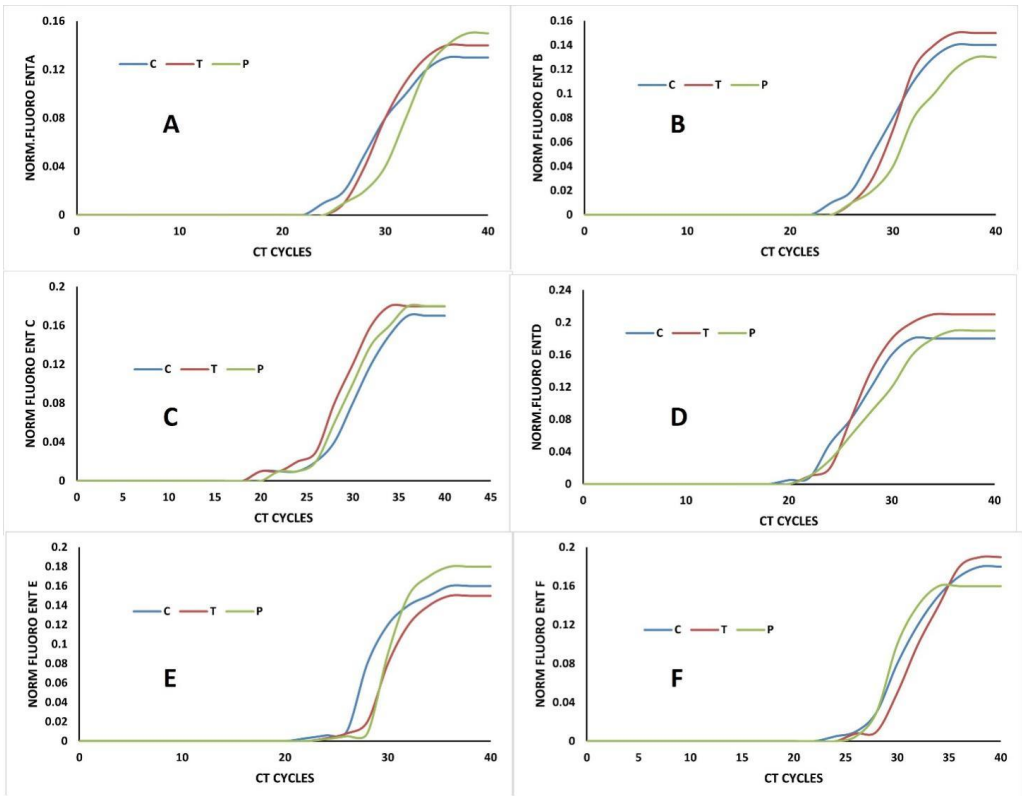

Figure 9. Ct curves: Ct values of the gene members in the study: (A) *entA*; (B) *entB*; (C) *entC*; (D) *entD*; (E) *entE*; (F) *entF*

4. DISCUSSION

Most community-acquired and hospital-associated cases of UTIs are caused by UPEC, which is the world's most common cause of UTIs. With the increasing antibiotic resistance patterns in UPEC strains, treatment is becoming more challenging, leading to frequent UTIs, which makes an extended hospital stay mandatory. This also makes patients receive multiple antibiotic treatments and invasive procedures [30]. Biofilm development and efflux pump activation are only a few of the resistance mechanisms that UPEC exhibits. These systems, which permit survival under antimicrobial pressure, hinder eradication efforts. The wider problem of antimicrobial resistance (AMR) is reflected in the rise of UPEC strains that are resistant to several medications. Since UTIs are among the most common bacterial illnesses, resistant UPEC strains act as a sentinel indication of the rate at which AMR is spreading [31]. The leading cause of UTIs among Iraqi patients is found to be UPEC, which now has a high incidence of MDR strains, which are reported in more than 50–90% of published studies. About 30% to 75% of UTIs are caused by UPEC; research indicates that the prevalence is higher in females (up to 90% in some studies). According to research conducted in 2024, 52.2% of samples in Baghdad alone tested positive for substantial bacteriuria, with *E. coli* being the most common infection at 63.2%. According to research from 2022, even Southern Iraq had a 30% UPEC prevalence and strong resistance patterns [32].

To scavenge iron, a vital material that is rare in the urinary system and necessary for UPEC proliferation and pathogenicity, UPEC creates enterobactin (Ent) in urine. Despite being targeted by the host defense protein lipocalin-2, Ent, a strong siderophore with a very high affinity for iron, is produced in urine and is vital for survival. It is frequently employed in conjunction with its modified version, salmochelin [33]. UPEC steals iron (III) from host proteins in the urine by employing enterobactin. Both during experim*entA*l infection and in the urine of UTI patients, enterobactin and its associated breakdown products are found. Enterobactin production is essential for UPEC's high-affinity iron collection in the nutrient-limited environment of the human bladder, despite its metabolic cost [34].

MG, a naturally occurring phenolic chemical that has antibacterial potential, including against drug-resistant forms. It works by lowering virulence, breaking up biofilms, and preventing bacterial growth. It is reported to be effective against *Pseudomonas aeruginosa*, *Staphylococcus aureus* (including MRSA), *Salmonella* spp., and *E. coli*. Additionally, it is claimed that MG increases the effectiveness of traditional antibiotics (such as nalidixic acid and ciprofloxacin) against resistant infections, frequently reinstating their activity [35]. The current investigation verified a 100% inhibition at roughly 80 µg/ml, which is significantly different from the PC ($p < 0.05$). After 24 h, MG decreased biofilm formation by 76% ($p < 0.05$), which is significant when compared to the PC's 89% inhibition at the same time ($p < 0.05$).

Galla Rhois contains a significant amount of MG, which is a good antibacterial against intestinal bacteria. The antibacterial properties of nalidixic acid when combined with MG were effective against nalidixic acid-resistant bacteria, as examined in a study by Choi et al. [36]. According to Kang et al. [37], MG may be utilized to stop the development of oral biofilms since it reduced the growth of oral pathogens and the production of S. mutans biofilms; however, Kacergius et al. [38] assessed the impact of sumac extract, particularly its bioactive component MG, on S. mutans biofilm production, employing an optical profilometry experiment. The anti-quorum-sensing (QS) effect of MG in *Pseudomonas aeruginosa* was initially reported by Hossain et al. [39]. Their study demonstrated that only MG showed a significant anti-QS effect out of the five phenolic compounds. They subsequently discovered that MG inhibited QS by interfering with the synthesis and activity of AHL. Recently, scientists have attempted to add antimicrobial compounds to d*entA*l adhesives. Epigallocatechin-3-gallate (EGCG) and epigallocatechin-3-O-(3-O-methyl)-gallate (EGCG-3Me) were added separately to the commercial adhesive Single Bond 2 (SB 2) at concentrations of 200, 400, and 600 µg/mL to screen for antibacterial properties [40].

The combined effects of MG and the antibiotic tylosin (Ty) on *Salmonella enterica* serovar Typhimurium, which causes intestinal infections in both humans and animals, were examined in a study by Mechesso et al. [41]. The study evaluated the bacterium's viability, membrane potential, cell integrity, and interactions with host cells, including adhesion, invasion, intracellular survival, and biofilm formation, when exposed to sub-inhibitory levels of MG. Davila-Avina et al. [42] assessed the effects of five phenolic compounds (PCs), including MG, on various traits of three pathotypes of *E. coli* (enteropathogenic, enterohemorrhagic, and enterotoxigenic). Growth, swarming movement, biofilm formation, and the expression of specific virulence genes were all investigated. When mixed with GA and tannic acid (TA), MG demonstrated bactericidal activity against all three pathotypes of *E. coli*. At low dosages, MG had the greatest impact on all strains. The enterobactin content decreased from 2.23 ± 0.14 (control) to 1.825 ± 0.41 at ½ MIC ($p < 0.05$). Conversely, at ½ MIC concentration, the PC displayed 1.092 ± 0.27 ($p < 0.05$). This demonstrates that MG may play a role in preventing the growth of bacteria. Similar findings were observed in the real-time-PCR gene expression study, which was carried out to assess the levels of *entA*, *entB*, *entC*, *entD*, *entE*, and *entF* gene expression. Following treatment with MG at ½ MIC, it was observed that all of the six gene members exhibited significant downregulation ($p < 0.05$).

Mohammed et al. [43] showed that certain plant-derived extracts and nanoparticles may dramatically lower the expression of the *Staphylococcus aureus* enterobactin genes (*entA*, *entB*, *entC*, and *entD*) using quantitative real-time polymerase chain reaction (qPCR). These virulence-associated genes, which are typically located on plasmids or pathogenicity islands, are essential for toxin production and pathogenicity. Their study highlighted the potential use of natural compounds and nanomaterials to interfere with bacterial gene regulation and hence decrease pathogenicity, rather than relying solely on bactericidal activity. Meanwhile, Nuñez et al. [44] reported that when methanol extracts were administered at sub-MIC dosages, they could either totally eliminate or drastically limit the synthesis of the *Staphylococcus aureus* enterobactin genes (*entA*, *entB*, *entC*, and *entD*). These genes, which are typically located on plasmids, are crucial for the production of toxins and pathogenicity. Pomegranate (*Punica granatum*) peel extracts operate as a potent, natural antibacterial agent against *Staphylococcus aureus*, inhibiting its proliferation and reducing the production of enterobactins. Methanolic peel extracts are very efficient against MRSA and have low MICs. These extracts have been shown to disrupt cell membranes,

reduce the formation of biofilms, and stop the production of staphylococcal enterobactin A (SEA) [45]. Enterobactin, a high-affinity iron-chelating siderophore, was produced by the *entC*EBA operon (*entA*, *entB*, *entC*, and *entD*) in *E. coli*. Downregulation of these gene members predicts that the bacteria could be overloaded with internal iron stores [46].

5. CONCLUSION

The present investigation describes the first use of manufactured MG against an isolate of UPEC. The findings revealed that the synthesis of MG blocked enterobactin formation. This was verified by real-time PCR, which showed downregulation of *entA*, B, C, D, E, and F gene members ($p < 0.05$). In a dose- and time-dependent manner, MG efficiently inhibits bacterial growth and biofilm formation against UPEC. Its potential as a therapeutic option is highlighted by its capacity to compromise membrane integrity and inhibit virulence factors. According to these findings, MG represents a promising natural compound requiring further investigation as a potential antimicrobial candidate.

ACKNOWLEDGMENT

The researchers would like to express their sincere appreciation and deep gratitude to the Department of Microbiology and the Department of Biology, College of Science, Mustansiriyah University, for their valuable support, scientific guidance, and continuous assistance throughout this study. Their cooperation and encouragement are highly appreciated.

REFERENCES

[1] Yang, X., Chen, H., Zheng, Y., Qu, S., Wang, H., Yi, F. (2022). Disease burden and long-term trends of urinary tract infections: A worldwide report. Frontiers in Public Health, 10: 888205. https://doi.org/10.3389/fpubh.2022.888205

[2] Abdul Hussein, M.T., Mohammed, B.B., Hamed, T.A. (2025). Chitosan-cryogels loaded with lactic acid bacteria supernatants effectively inhibit uropathogenic Escherichia coli biofilms and virulence. International Journal of Design & Nature and Ecodynamics, 20(11): 2545-2555. https://doi.org/10.18280/ijdne.201106

[3] Manges, A.R., Geum, H.M., Guo, A., Edens, T.J., Fibke, C.D., Pitout, J.D.D. (2019). Global extraintestinal pathogenic Escherichia coli lineages. Clinical Microbiology Reviews, 32. https://doi.org/10.1128/CMR.00135-18

[4] Gomes, T.A.T., Elias, W.P., Scaletsky, I.C.A., et al. (2016). Diarrheagenic Escherichia coli. Brazilian Journal of Microbiology, 47(Suppl 1): 3-30. https://doi.org/10.1016/j.bjm.2016.10.015

[5] Alshammary, R.A., Khadim, M.M., Al-Karawi, A.S., et al. (2025). Biomarkers of sepsis severity: A comparative evaluation of immunological and biochemical parameters. Al-Anbar Medical Journal, 21(4).

[6] Neupane, S., Pant, N.D., Khatiwada, S., Chaudhary, R., Banjara, M.R. (2016). Correlation between biofilm formation and resistance toward different commonly used antibiotics along with extended spectrum beta-lactamase production in uropathogenic Escherichia coli isolated from patients suspected of urinary tract infections visiting Shree Birendra Hospital, Chhauni, Kathmandu, Nepal. Antimicrobial Resistance & Infection Control, 5: 5. https://doi.org/10.1186/s13756-016-0104-9

[7] Khazaal, M.T., Faraag, A.H.I., Hamada, M.A., El-Hendawy, H.H. (2024). Characterization and statistical optimization of enterotoxin synthesized by Escherichia coli OQ866153. Biochemical Genetics, 62(5): 3920-3945. https://doi.org/10.1007/s10528-023-10626-z

[8] Schüroff, P.A., Abe, C.M., Silva, J.W., et al. (2022). Role of aggregate-forming pilus (AFP) in adherence and colonization of both intestinal and urinary tracts. Virulence, 13: 1423-1433. https://doi.org/10.1080/21505594.2022.2112818

[9] Kadry, A.A., Al-Kashef, N.M., El-Ganiny, A.M. (2020). Distribution of genes encoding adhesins and biofilm formation capacity among uropathogenic Escherichia coli isolates in relation to antimicrobial resistance. African Health Sciences, 20: 238. https://doi.org/10.4314/ahs.v20i1.29

[10] Wang, C., Li, Q., Lv, J., et al. (2020). Alpha-hemolysin of uropathogenic Escherichia coli induces GM-CSF-mediated acute kidney injury. Mucosal Immunology, 13: 22-33. https://doi.org/10.1038/s41385-019-0225-6

[11] Carlini, F., Maroccia, Z., Fiorentini, C., Travaglione, S., Fabbri, A. (2021). Effects of the Escherichia coli bacterial toxin cytotoxic necrotizing factor 1 on different human and animal cells: A systematic review. International Journal of Molecular Sciences, 22: 12610. https://doi.org/10.3390/ijms222212610

[12] Massip, C., Oswald, E. (2020). Siderophore-microcins in Escherichia coli: Determinants of digestive colonization, the first step toward virulence. Frontiers in Cellular and Infection Microbiology, 10: 381. https://doi.org/10.3389/fcimb.2020.00381

[13] Hood, M.I., Skaar, E.P. (2012). Nutritional immunity: Transition metals at the pathogen-host interface. Nature Reviews Microbiology, 10(8): 525-537. https://doi.org/10.1038/nrmicro2836

[14] Kramer, J., Özkaya, Ö., Kümmerli, R. (2020). Bacterial siderophores in community and host interactions. Nature Reviews Microbiology, 18(3): 152-163. https://doi.org/10.1038/s41579-019-0284-4

[15] Gould, D. (2010). Causes, prevention, and treatment of Escherichia coli infections. Nursing Standard, 24(31): 50. https://doi.org/10.7748/ns2010.04.24.31.50.c7692

[16] Mühlen, S., Dersch, P. (2016). Anti-virulence strategies to target bacterial infections. In How to Overcome the Antibiotic Crisis: Facts, Challenges, and Technological Future Perspectives, pp.147-183.

[17] Dickey, S.W., Cheung, G.Y.C., Otto, M. (2017). Different drugs for bad bugs: Antivirulence strategies in the age of antibiotic resistance. Nature Reviews Drug Discovery, 16(7): 457-471. https://doi.org/10.1038/nrd.2017.23

[18] Wang, M., Li, H. (2025). Structure, function, and biosynthesis of siderophores produced by Streptomyces species. Journal of Agricultural and Food Chemistry, 73(8): 4425-4439. https://doi.org/10.1021/acs.jafc.4c08231

[19] Gehring, A.M., Mori, I., Walsh, C.T. (1998).

Reconstitution and characterization of the Escherichia coli enterotoxin synthetase from EntB, EntE, and EntF. Biochemistry, 37(8): 2648-2659. https://doi.org/10.1021/bi9726584
[20] Gorshkov, V., Parfirova, O., Petrova, O., et al. (2021). The knockout of enterotoxin-related genes in Pectobacterium atrosepticum results in reduced stress resistance and virulence toward primed plants. International Journal of Molecular Sciences, 22(17): 9594. https://doi.org/10.3390/ijms22179594
[21] Sargun, A., Johnstone, T.C., Zhi, H., et al. (2021). Enterobactin- and salmochelin-β-lactam conjugates induce cell morphologies consistent with inhibition of penicillin-binding proteins in uropathogenic Escherichia coli CFT073. Chemical Science, 12(11): 4041-4056. https://doi.org/10.1039/D0SC04337K
[22] Prakashkumar, N., Sivamaruthi, B.S., Chaiyasut, C., Suganthy, N. (2021). Decoding the neuroprotective potential of methyl gallate-loaded starch nanoparticles against beta amyloid-induced oxidative stress-mediated apoptosis: An in vitro study. Pharmaceutics, 13(3): 299. https://doi.org/10.3390/pharmaceutics13030299
[23] Ugbo, E., Anyamene, C., Moses, I., et al. (2020). Prevalence of blaTEM, blaSHV, and blaCTX-M genes among extended spectrum beta-lactamase-producing Escherichia coli and Klebsiella pneumoniae of clinical origin. Gene Reports, 21: 100909.
[24] Said-Salman, I.H., Jebaii, F.A., Yusef, H.H., et al. (2019). Global gene expression analysis of Escherichia coli K-12 DH5α after exposure to 2.4 GHz wireless fidelity radiation. Scientific Reports, 9: 14425. https://doi.org/10.1038/s41598-019-51046-7
[25] Irayyif, S.M., Araghi, A.M.S., Malla, S. (2015). Silver nanoparticles and their effect on biofilm formation in foodborne Salmonella species. International Journal of Recent Scientific Research, 6: 4343-4346.
[26] Oh, S.J., Kim, H., Liu, Y., et al. (2014). Incompatibility of silver nanoparticles with lactate dehydrogenase leakage assay for cellular viability test is attributed to protein binding and reactive oxygen species generation. Toxicology Letters, 225(3): 422-432. https://doi.org/10.1016/j.toxlet.2014.01.015
[27] Venkatasubbu, G.D., Baskar, R., Anusuya, T., Seshan, C.A., Chelliah, R. (2016). Toxicity mechanism of titanium dioxide and zinc oxide nanoparticles against food pathogens. Colloids and Surfaces B: Biointerfaces, 148: 600-606.
[28] Ma, L., Payne, S.M. (2012). AhpC is required for optimal production of enterotoxin by Escherichia coli. Journal of Bacteriology, 194(24): 6748-6757. https://doi.org/10.1128/JB.01574-12
[29] Said-Salman, I.H., Jebaii, F.A., Yusef, H.H., et al. (2019). Global gene expression analysis of Escherichia coli K-12 DH5α after exposure to 2.4 GHz wireless fidelity radiation. Scientific Reports, 9: 14425. https://doi.org/10.1038/s41598-019-51046-7
[30] Naskar, M., Choi, H.W. (2024). A dynamic interplay of innate immune responses during urinary tract infection. Immune Network, 24(4): e31. https://doi.org/10.4110/in.2024.24.e31
[31] Terlizzi, M.E., Gribaudo, G., Maffei, M.E. (2017). UroPathogenic Escherichia coli (UPEC) infections: Virulence factors, bladder responses, antibiotic, and non-antibiotic antimicrobial strategies. Frontiers in Microbiology, 8: 1566. https://doi.org/10.3389/fmicb.2017.01566
[32] Salman, H.S., Majeed, H.M., Shallal, Y.F. (2026). Prevalence, etiology, and antibiotic resistance patterns of urinary tract infections in a Baghdad hospital: Focus on uropathogenic E. coli and virulence factors. International Journal of Microbiology, 2026: 9117996. https://doi.org/10.1155/ijm/9117996
[33] Zou, Z., Robinson, J.I., Steinberg, L.K., Henderson, J.P. (2023). Uropathogenic Escherichia coli wield enterotoxin-derived catabolites as siderophores. bioRxiv, 2023: 2023.07.25.550588. https://doi.org/10.1101/2023.07.25.550588
[34] Shields-Cutler, R.R., Crowley, J.R., Miller, C.D., Stapleton, A.E., Cui, W., Henderson, J.P. (2016). Human metabolome-derived cofactors are required for the antibacterial activity of siderocalin in urine. Journal of Biological Chemistry, 291: 25901-25910.
[35] Flores-Maldonado, O., Dávila-Aviña, J., González, G.M., Becerril-García, M.A., Ríos-López, A.L. (2025). Antibacterial activity of gallic acid and methyl gallate against emerging non-fermenting bacilli. Folia Microbiologica, 70(1): 127-135. https://doi.org/10.1007/s12223-024-01182-z
[36] Choi, J.G., Kang, O.H., Lee, Y.S., et al. (2009). Antibacterial activity of methyl gallate isolated from Galla Rhois or carvacrol combined with nalidixic acid against nalidixic acid-resistant bacteria. Molecules, 14(5): 1773-1780. https://doi.org/10.3390/molecules14051773
[37] Kang, M.S., Oh, J.S., Kang, I.C., et al. (2008). Inhibitory effect of methyl gallate and gallic acid on oral bacteria. Journal of Microbiology, 46: 744-750. https://doi.org/10.1007/s12275-008-0235-7
[38] Kacergius, T., Abu-Lafi, S., Kirkliauskiene, A., et al. (2017). Inhibitory capacity of Rhus coriaria L. extract and its major component methyl gallate on Streptococcus mutans biofilm formation by optical profilometry: Potential applications for oral health. Molecular Medicine Reports, 16:949-956. https://doi.org/10.3892/mmr.2017.6674
[39] Hossain, M.A., Lee, S.J., Park, N.H., et al. (2017). Impact of phenolic compounds in the acyl homoserine lactone-mediated quorum sensing regulatory pathways. Scientific Reports, 7: 10618. https://doi.org/10.1038/s41598-017-10997-5
[40] Yu, H.H., Zhang, L., Yu, F., Li, F., Liu, Z.Y., Chen, J.H. (2017). Epigallocatechin-3-gallate and epigallocatechin-3-O-(3-O-methyl)-gallate enhance the bonding stability of an etch-and-rinse adhesive to dentin. Materials, 10: 183. https://doi.org/10.3390/ma10020183
[41] Mechesso, A.F., Yixian, Q., Park, S.C. (2019). Methyl gallate and tylosin synergistically reduce membrane integrity and intracellular survival of Salmonella Typhimurium. PLoS ONE, 14: e0221386. https://doi.org/10.1371/journal.pone.0221386
[42] Davila-Avina, J., Gil-Solis, C., Merino-Mascorro, J., Garcia, S., Heredia, N. (2020). Phenolics with bactericidal activity alter motility and biofilm formation in entErotoxigenic, entEropathogenic, and entErohemorrhagic Escherichia coli. Foodborne Pathogens and Disease, 17: 568-575. https://doi.org/10.1089/fpd.2019.2766
[43] Mohammed, S.A., Al-Ani, M.I.J., Mohammed, D.L.,

Salar, L.R., Rasul, B.M. (2018). Inhibition of Staphylococcus aureus enterotoxin genes by employing plant extracts. Innovaciencia, 6(2): 1-8. https://doi.org/10.15649/2346075X.469

[44] Nuñez, L., D'Aquino, M. (2012). Microbicide activity of clove essential oil (Eugenia caryophyllata). Brazilian Journal of Microbiology, 43(4): 1255-1260. https://doi.org/10.1590/S1517-83822012000400003

[45] Braga, L.C., Shupp, J.W., Cummings, C., et al. (2005). Pomegranate extract inhibits Staphylococcus aureus growth and subsequent enterotoxin production. Journal of Ethnopharmacology, 96(1-2): 335-339. https://doi.org/10.1016/j.jep.2004.08.034

[46] Amiri, M., Golchin, M., Jamshidian Mojaver, M., Farzin, H., Hajizade, A. (2025). EntErobactin: A key player in bacterial iron acquisition and virulence and its implications for vaccine development and antimicrobial strategies. Virulence, 16(1): 2563018. https://doi.org/10.1080/21505594.2025.2563018